

# Copolymerization of $\alpha$ -Cyanovinyl Acetate with Acrylonitrile and Methacrylonitrile: Synthesis, Characterization, and Study of their Dielectric Behavior

Mourad Arous,<sup>1</sup> Ali Kallel,<sup>1</sup> Hamid Kaddami,<sup>2</sup> Mohamed Lahcini,<sup>2</sup>  
Ahmed Belfkira,<sup>2</sup> Mustapha Raihane<sup>2</sup>

<sup>1</sup>Laboratoire des Matériaux Composites, Céramiques et Polymères, Faculté des Sciences de Sfax, Route de Skoura, Sfax 3018, Tunisia

<sup>2</sup>Laboratoire de Chimie Bioorganique et Macromoléculaire, Faculté des Sciences et Techniques, Avenue Abdelkrim Khattabi, BP 549, Marrakech 40000, Morocco

Received 3 October 2007; accepted 22 April 2009

DOI 10.1002/app.30747

Published online 16 June 2009 in Wiley InterScience (www.interscience.wiley.com).

**ABSTRACT:** In the frame of a research aiming at developing new dielectric polymers containing C—CN substituent with strong dipole moment, the radical copolymerization of cyano (nitrile) monomers and an  $\alpha$ -cyanovinyl acetate (CVA) as the comonomer, initiated by AIBN is described. Methacrylonitrile (MAN) and acrylonitrile (AN) were chosen as the cyano monomers. The homopolymer of CVA was also prepared and the corresponding yield was close to 60%. All these polymers were characterized by <sup>13</sup>C NMR, IR, DSC, and TGA. The percentages of incorporation of AN and MAN in the copolymers were 36 and 56%, respectively. These products showed high glass transition temperatures,  $T_g$ , ranging between 124 and 142°C. The thermogravimetry analyses showed that these copolymers are stable up to 200°C. Dielectric spectroscopy analysis revealed a weak relaxation  $\beta$  process below  $T_g$ . The  $\alpha$  relaxation phenomena

have also been characterized around the  $T_g$  and associated to the cooperative movements of the polar groups (CN). The values of dielectric relaxation increment were calculated at 150°C using the Havriliak–Negami equation and indicated that these polymers exhibit interesting dielectric properties comparatively to similar cyano materials. The  $\alpha$ -activation energies were also calculated. New statistic copolymers based on CVA were characterized. The values of the intensity of  $\alpha$  relaxation show the potential application of such materials in the domain of electronics. © 2009 Wiley Periodicals, Inc. *J Appl Polym Sci* 114: 1094–1104, 2009

**Key words:**  $\alpha$ -cyanovinyl acetate copolymers; radical copolymerization; NMR spectroscopy; thermal properties; dielectric relaxations

## INTRODUCTION

Vinylidene cyanide (VCN) is known to polymerize with a wide variety of monomers, such as vinyl acetate, styrene, or dienes, to form chiefly alternating copolymers.<sup>1</sup> Their mechanical properties have been studied extensively.<sup>2</sup> New applications of VCN were found by Miyata et al.<sup>3</sup> who observed piezoelectric properties for the amorphous copolymer of VCN with vinyl acetate. Therefore, studies that include the copolymerization reactions of VCN with various monomers have been of growing relevance in the last few years. VCN copolymerized with methyl methacrylate,<sup>4</sup> isopropenyl acetate,<sup>5</sup> vinyl benzoate,<sup>6</sup> styrene,<sup>4</sup> substituted styrenes,<sup>7</sup> and vinyl esters of fatty acids.<sup>8</sup> All these copolymerizations gave

alternating copolymers, and their microstructures were characterized by <sup>13</sup>C NMR spectroscopy.

Fundamental studies of the piezoelectric properties of some copolymers take into account the chain mobility in the macromolecules,<sup>9</sup> their dielectric properties,<sup>10,11</sup> and their enthalpy relaxation.<sup>12</sup> Industrial patents report the main characteristic of piezoelectric copolymers of vinylidene cyanide.<sup>13,14</sup>

Other cyano monomers such as methacrylonitrile (MAN) and acrylonitrile (AN) copolymerized with vinyl or isopropenyl acetate and with vinyl formate.<sup>15</sup> The resulting copolymers showed interesting pyroelectric properties.<sup>16</sup> In addition, copolymers based on methylvinylidene cyanide and vinyl acetate<sup>17</sup> or styrene<sup>7</sup> exhibit interesting dielectric behavior.<sup>18</sup>

The properties of copolymers containing cyano groups can be improved with a higher concentration of dipoles along the chains. The copolymerization reaction of cyano monomers with captodative monomers (such as 1,1-disubstituted ethylene having an electron-withdrawing (capto) and an electron-donor (dative) substituent on the same carbon) could provide new materials with potential electric properties.

Correspondence to: M. Raihane (raihanem@yahoo.fr).

Contract grant sponsor: Morocco and Tunisia committee in the frame of the program of collaboration of exchange scientific; contract grant number: 28/02.

VCN copolymerized with captodative monomers such as  $\alpha$ -cyanovinyl acetate and methacrylonitrile.<sup>19</sup> Statistical copolymers based on acrylonitrile and methacrylonitrile with ethyl  $\alpha$ -acetoxyacrylate<sup>20</sup> and methyl  $\alpha$ -acetoxy acrylate<sup>21</sup> were synthesized by radical copolymerization. The microstructure of the resulting copolymers was characterized by <sup>13</sup>C NMR, and some reactivity ratios could be assessed. The copolymers of vinylidene cyanide exhibit a highly alternating structure in contrast to those of copolymers based on methacrylonitrile and acrylonitrile, which were more statistic than alternating.

Recently, the copolymers based on cyano monomers such as AN or MAN or methyl vinylidene cyanide (MVCN), and 2,2,2-trifluoroethyl methacrylate comonomer were synthesized by radical process initiated by AIBN. These copolymers were characterized by <sup>1</sup>H, <sup>13</sup>C, <sup>19</sup>F NMR, and IR spectroscopy.<sup>22</sup>

To develop new dielectric polymers containing CN substituents with strong dipole moments, we describe in this article the radical copolymerization of AN or MAN with  $\alpha$ -cyanovinyl acetate (CVA) and their dielectric behavior.

## EXPERIMENTAL

### Materials

Methacrylonitrile (MAN) (bp: 90–92°C/ 760 mm Hg), acrylonitrile (AN) (bp: 77°C/ 760 mm Hg), and  $\alpha$ -cyanovinyl acetate (CVA) (bp: 80–82°C/ 30 mm Hg) are commercially available products (Aldrich Chimie) and were distilled under reduced pressure, then stored below 5°C before use.  $\alpha,\alpha'$ -Azobisisobutyronitrile (AIBN) was provided by Aldrich and was purified by recrystallisation from ethanol. Acetonitrile of analytical grade (Aldrich) was distilled over calcium hydride before use.

### Synthesis

Radical homopolymerization of  $\alpha$ -cyanovinyl acetate (CVA) was performed in acetonitrile in glass tube using AIBN as the initiator.

The radical copolymerization of cyano monomers (AN or MAN) and CVA were performed in thick borosilicate Carius tubes (length 130 mm, internal diameter 10 mm, thickness 2.5 mm, and total volume 8 cm<sup>3</sup>). After introducing initiator (AIBN, 1 wt % relative for the monomer mixture), cyano monomer, CVA, and acetonitrile under inert atmosphere, the tube was connected to a vacuum line and purged several times by evacuating and flushing with helium. After six thaw-freeze cycles to remove oxygen, the tube was cooled into liquid nitrogen, sealed under vacuum, and placed into a shaking oven heated at 80°C for 12 h. After reaction, the tube was

cooled into liquid nitrogen, opened, and the total product mixture was solubilized in *N,N*-dimethylformamide and then precipitated from methanol. The powder formed was isolated by filtration and dried under vacuum at 80°C for 24 h.

### Characterization

NMR were recorded on a Bruker (Wissembourg, France) AM 300 spectrometer (300 and 75 MHz, for <sup>1</sup>H and <sup>13</sup>C, respectively) using dimethyl sulfoxide DMSO-d<sub>6</sub> as the solvent and TMS as the internal standard.

Infrared spectroscopy measurements were performed in transmittance with a spectrometer Nicolet 510 P from samples in KBr disks. The accuracy was  $\pm 2$  cm<sup>-1</sup>.

Differential scanning calorimetry (DSC) measurements were conducted using a Perkin-Elmer Pyris 1 instrument connected to a microcomputer. The apparatus was calibrated with indium and *n*-decane. After its insertion into the DSC apparatus, the sample was cooled initially to -100 °C for 15 min. Then, the first scan was made at a heating rate of 20°C min<sup>-1</sup> up to 100°C, where it remained for 2 min. It was then cooled to -100°C at the rate of 320°C min<sup>-1</sup> and left for 10 min at this temperature before a second scan was started at a heating rate of 20°C min<sup>-1</sup>, giving the values of  $T_g$  reported herein, taken at the half-height of the capacity jump of the glass transition.

Thermogravimetry analyses were performed with a Texas Instrument TGA 51–133 apparatus under nitrogen with a heating rate of 10°C min<sup>-1</sup> from room temperature up to 550°C.

Dielectric relaxation spectroscopy (DRS) measurements were performed on thin rectangular strips (dimensions of about 10 × 10 × 0.5 mm<sup>3</sup>). The films were metalized using aluminum to prevent the specimen from losing its dimensional integrity when heating and to improve the contact with the electrodes. Then, the sample was placed between two gold parallel plate electrodes. The parallel plate sensors were used to evaluate bulk dielectric properties and to track molecular relaxations.

Dielectric determinations of the complex permittivity  $\epsilon^*$

$$\epsilon^* = \epsilon'(f) - j\epsilon''(f)$$

were performed on a dielectric thermal analyzer DEA 2970 from TA Instruments allowing measurements over the temperature ranging from -150°C to 300°C and a frequency interval from 0.001 to 100 kHz. A platinum resistance temperature detector (RTD) surrounds the perimeter of the gold electrode and measures the temperature of the sample. The

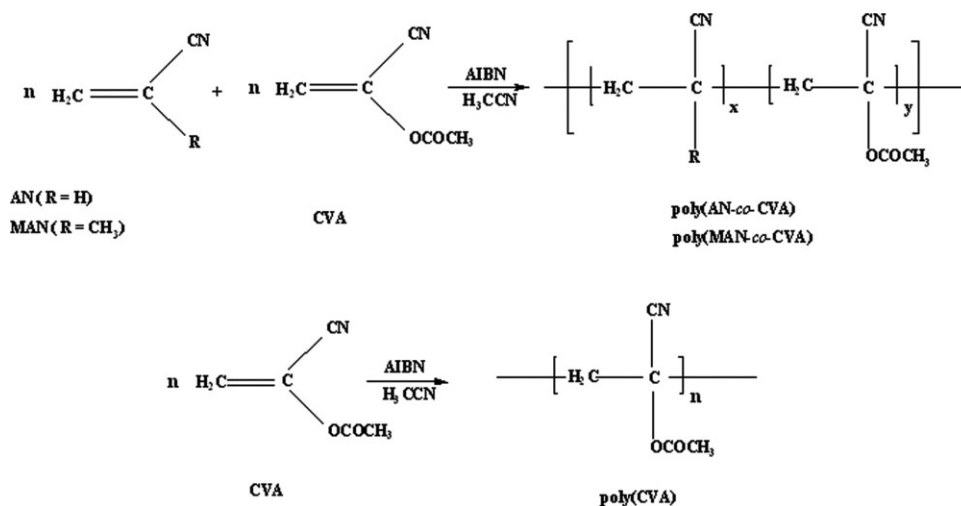


Figure 1 Synthetic routes of copolymers based on CVA.

temperature is controlled directly by the RTD. Two types of dielectric measurements were performed by isochronal runs with fixed frequencies and ramping temperatures from ambient to 170°C, and then decreasing it with a heating rate of 2°C min<sup>-1</sup> under a nitrogen atmosphere on one hand, or by isothermal runs with fixed temperature and scanning frequencies on the other hand.

## RESULTS AND DISCUSSION

Original cyano copolymers bearing nitrile (or cyano) groups were synthesized by radical copolymerization of equimolar proportions of  $\alpha$ -cyanovinyl acetate (CVA) with nitrile monomers (acrylonitrile: AN and methacrylonitrile: MAN) mixed with 1 wt % of initiator (AIBN) in acetonitrile as solvent (Fig. 1, Table I). These reactions were initiated by AIBN at 80°C. After reaction and purification by precipitation, these polymers obtained in 40–60% yields were characterized by NMR spectroscopy, and their thermal and dielectric properties were investigated.

## Spectroscopic characterizations and microstructures

The IR spectrum of poly(CVA) showed characteristic bands at 2953 cm<sup>-1</sup> (aliphatic C–H stretch), 2243 cm<sup>-1</sup> (C≡N stretch), 1765 cm<sup>-1</sup> (C=O) and 1271–1020 cm<sup>-1</sup> (C–O).

Similar observations can be noted for the IR spectrum of poly(AN-co-CVA) copolymer. The vinylic bond absorbances (C=C) of CVA and of AN at 1635 cm<sup>-1</sup> and 1620 cm<sup>-1</sup>,<sup>22,23</sup> respectively, are absent, indicating that the copolymerization reaction occurred. The characteristic bands of this copolymer are 2940 cm<sup>-1</sup> (aliphatic C–H stretch), 2246 cm<sup>-1</sup> (C≡N stretch), 1755 cm<sup>-1</sup> (C=O), 1435–1372 cm<sup>-1</sup> (out-of-plane C–H) and 1211–1120 cm<sup>-1</sup> (C–O).

Table II summarizes the 75 MHz <sup>13</sup>C NMR chemical shifts of the different groups observed in the spectra of poly(CVA) and two copolymers of CVA. For example, the <sup>13</sup>C NMR spectra of poly(AN-co-CVA) and poly(MAN-co-CVA) copolymers are given in Figures 2 and 3, respectively.

The assignments were deduced from the comparison with those of the homopolymers of cyano monomers,<sup>23–25</sup> poly(CVA) homopolymer and poly(VCN-co-CVA) copolymer.<sup>19</sup> The spectra showed

TABLE I  
Monomer/copolymer Composition of the Polymers of CVA and Their Glass Transition and Decomposition Temperatures

(Co)Polymer	CVA in feed		CVA in copolymer		
	Mol%	Mol%	$T_g$ (°C)	$T_d$ (°C) <sup>a</sup>	$T_d$ (°C) <sup>b</sup>
Poly(CVA)	100	100	124	200	244
Poly(AN-co-CVA)	50	63	142	208	256
Poly(MAN-co-CVA)	50	44	129	212	265

Polymers heated under nitrogen at 10°C min<sup>-1</sup>.

<sup>a</sup>  $T_d$ : Temperature of beginning of degradation at 1% of loss weight.

<sup>b</sup>  $T_d$ : Temperature of degradation at 10% of loss weight.

TABLE II  
Assignments of  $^{13}\text{C}$  NMR Chemical Shifts /ppm for Poly(CVA) and the Copolymers of CVA

Type de carbon	Poly(CVA)	Poly(AN-co-CVA)	Poly(MAN-co-CVA)
CH <sub>2</sub> (main chain)	42.6 – 44.0	42.0	42.5–47.3
CH(AN)	—	34.0	—
CH <sub>3</sub> (CVA)	20.5	20.5–21.7	21.0
CH <sub>3</sub> (MAN)	—	—	23.8–26.1
CO (CVA)	168.0	168.8	168.7
CN (MAN or AN)	—	119.1–121.2	122.5–123.8
CN (CVA)	115.1 – 115.4	115.3–116.6	115.2–117.6
C(CH <sub>3</sub> ) (MAN)	—	—	30.7–33.1
C(CN) (CVA)	67.3–67.6	67.0–72.9	67.3–70.0

the chemical shifts of different carbon atoms in the copolymers. Peaks assigned to vinylic carbons (the H<sub>2</sub>C=C at 136.8 ppm for AN; 132 ppm for MAN and 132 ppm for CVA and the H<sub>2</sub>C=C(CN)— at 107 ppm for AN; 118 ppm for MAN and 118.6 ppm for CVA, respectively) were absent in these spectra.

The composition of the copolymers can be assessed from the integrals of some characteristic peaks in the  $^{13}\text{C}$  NMR spectra. For the poly(MAN-co-CVA) copolymer, the areas of the signals of monomers incorporated were calculated by measuring the integrals of signals in  $^{13}\text{C}$  NMR spectrum of CN group of MAN ( $I_1$ ) in the range 122.5–123.8 ppm and the CN group of CVA ( $I_2$ ) in the 115.2–117.6 ppm range, using the following relation:

$$\text{mol \% MAN in the copolymer} = \frac{I_1}{I_1 + I_2} \times 100 \quad (1)$$

Starting from a molar feed composition of 1 : 1 for CVA : MAN, the copolymer contained approxi-

mately a 44 : 56 mol. ratio of CVA : MAN. The copolymerization composition of MAN with methyl  $\alpha$ -acetoxy acrylate was calculated using elemental analysis, and the incorporation of MAN was close to 50%.<sup>21</sup> The expansion of the resonance of the quaternary carbon in the  $^{13}\text{C}$  NMR spectrum of poly(MAN-co-CVA) copolymer in the region 30.5–33.0 ppm can explain the microstructure. Three main peaks are observed for the quaternary carbon atom of MAN unit at 31.5, 32.0 and 32.4 ppm (Fig. 2) and can be respectively corresponding to mm, mr and rr triads centered in MAN unit.<sup>21,22</sup> A similar result was observed for the resonance of nitrile group of MAN unit with chemical shifts at 122, 122.6, and 123.4 ppm (Fig. 2). The triads concentration for syndiotactic (rr), atactic (mr), and isotactic (mm) can be assessed from numerical integral of the resonance from CN of MAN.<sup>26</sup> We obtained 15% (rr), 50% (mr) and 35% (mm). In the alternating copolymers of poly(VCN-alt-methyl  $\alpha$ -acetoxyacrylate),<sup>21,26</sup> and

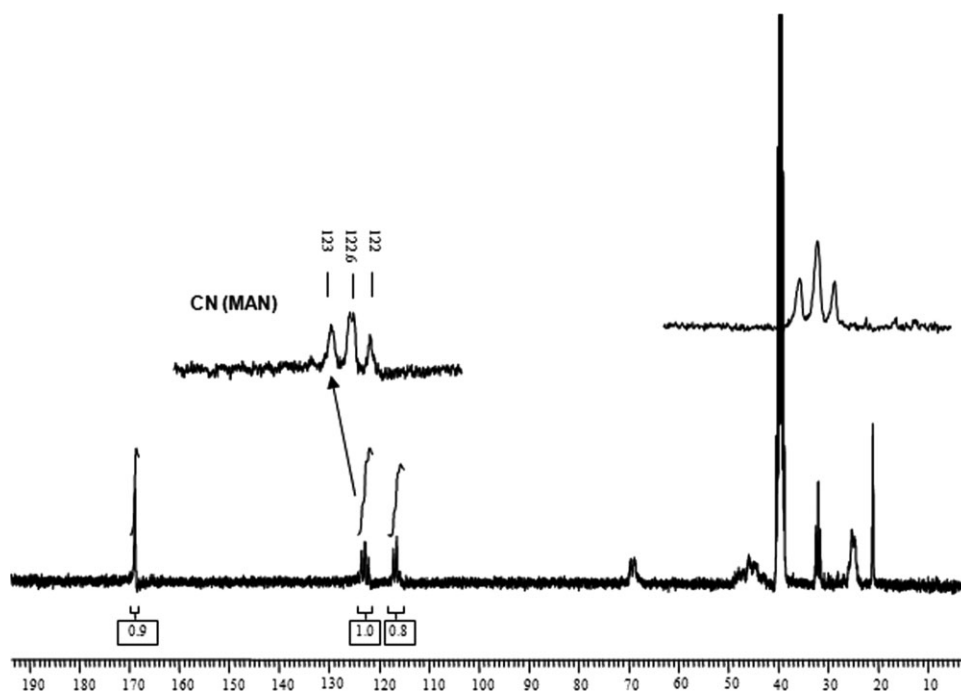
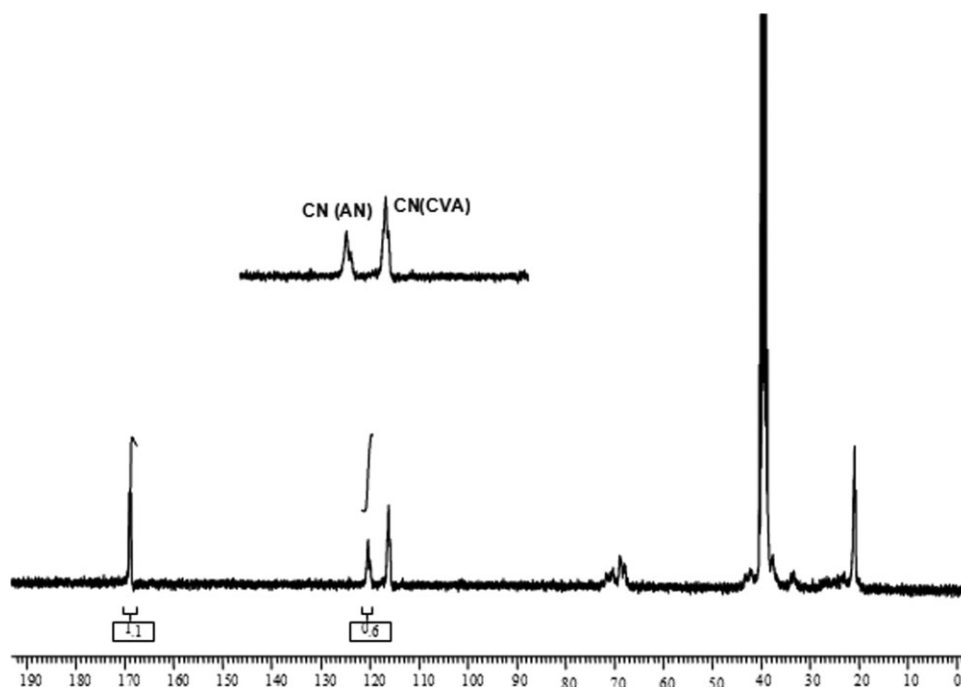


Figure 2  $^{13}\text{C}$  NMR spectrum of poly(MAN-co-CVA) copolymer recorded in deuterated DMSO-d<sub>6</sub>.





**Figure 3**  $^{13}\text{C}$  NMR spectrum of poly(AN-*co*-CVA) copolymer recorded in deuterated DMSO- $\text{d}_6$ .

poly(VCN-*alt*-methyl methacrylate),<sup>4</sup> the resonance of the carbon atom in cyanide group of MAN showed three broad peaks in 25 %: 50 %: 25% ratio arising from the triad sequences centered in VCN. The nature and the shape of the peaks of the CN of MAN in the poly(MAN-*co*-CVA) copolymer does not suggest an alternating structure. Therefore, poly(MAN-*co*-CVA) copolymer could exhibit a statistical structure corresponding to an alternating structure with homopolymer sequences of MAN and/or CVA as it was observed in similar copolymers based on MAN.<sup>21,22</sup>

The composition of the poly(AN-*co*-CVA) copolymer can also be assessed by measuring areas of the CN group of CVA unit ( $I_1 = 1.0$ ) and to the CN of the AN unit ( $I_2 = 0.6$ ) from  $^{13}\text{C}$  NMR. The molar percentage of incorporated AN in the copolymer is close to 37% (63% of CVA). This result was observed in the poly(AN-*stat*-methyl  $\alpha$ -acetoxyacrylate) copolymer.<sup>21</sup> As for the previous poly(MAN-*co*-CVA) copolymer, examination of CN region can give information about the microstructure of the product. Two groups of broad peaks in the 115.3–116.6 and 119.1–121.2 ppm ranges were not well separated (Fig. 3). Therefore, the poly(AN-*co*-CVA) could be mostly statistical.

The results of the Alfrey–Price Q–e parameters<sup>27</sup> where Q and e take into account the stabilization by resonance and the polar effects of the monomer scheme respectively are commonly used to predict the monomer reactivity ratios. The Alfrey – Price parameters are known for AN ( $Q_1 = 0.48$ ,  $e_1 = 1.24$ ),

MAN ( $Q_1 = 0.85$ ,  $e_1 = 0.79$ )<sup>28</sup> and CVA ( $Q_2 = 1.17$ ,  $e_2 = 1.06$ ).<sup>29</sup> The calculated values of the reactivity ratios  $r_1$  of cyano monomer and the  $r_2$  of CVA were determinate from the Alfrey–Price equations. Table III gives the calculated values of the reactivity ratios, the product ( $r_1 \times r_2$ ) and  $1/r_2$ .

The values of the product ( $r_1 \times r_2$ ) for the copolymers of CVA (Table III) are higher than zero, explaining the statistical structure. In poly(MAN-*co*-CVA) copolymer, this product was equal to 0.49. Similar result was observed in the statistical poly(MAN-*stat*-methyl  $\alpha$ -acetoxyacrylate) copolymer with the value of the product ( $r_1 \times r_2$ ) closing to 0.48 using Kelen–Tüdös method.<sup>26</sup> This result was in good agreement with the NMR characterization above.

The reactivity ratio  $r_2$  of CVA is defined as the ratio between the homopolymerization rate constant of CVA ( $k_{22}$ ) and the propagation rate of CVA radical onto AN or MAN monomer ( $k_{21}$ ). The higher value of  $1/r_2$  for poly(MAN-*co*-CVA) comparatively to the poly(AN-*co*-CVA) copolymer indicated that MAN monomer is more reactive than the AN

**TABLE III**  
Reactivity Ratios of Cyano Monomers ( $r_1$ ) and CVA ( $r_2$ ) and the Values of the Product ( $r_1 \times r_2$ ) and  $1/r_2$  Calculated from the Alfrey –Price Parameters

Copolymers	$r_1$	$r_2$	$r_1 \times r_2$	$1/r_2$
Poly(AN- <i>co</i> -CVA)	0.33	2.95	0.97	0.34
Poly(MAN- <i>co</i> -CVA)	0.89	0.55	0.49	1.83

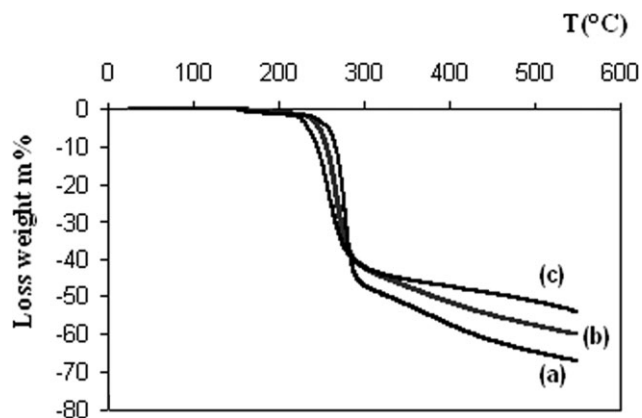


**Figure 4** TGA thermograms under nitrogen of poly(CVA) and copolymers of CVA: (a) poly(CVA) homopolymer, (b) poly(AN-co-CVA) copolymer, and (c) poly(MAN-co-CVA) copolymer.

monomer towards to CVA radicals. This result explains that the percentage of incorporation of MAN in the poly(MAN-co-CVA) copolymer is higher than the composition of AN in poly(AN-co-CVA) copolymer calculated from  $^{13}\text{C}$  NMR characterization.<sup>22</sup>

### Thermal properties

Two keys thermal properties were studied, glass transition temperature  $T_g$  and thermal degradation,  $T_{\text{dec}}$ , determined by differential scanning calorimetry (DSC) and by thermogravimetry analysis (TGA), respectively.

All the polymers analyzed show a sharp transition from the glassy domain to the viscoelastic one, as evidenced by the presence of only a neat  $T_g$  (Table I). It indicates that the polymer exhibited amorphous behavior with high  $T_g$  temperatures.

Higher  $T_g$  of the poly(AN-co-CVA) and poly(MAN-co-CVA) copolymers in comparison with that of poly(CVA) homopolymer ( $T_g = 124^\circ\text{C}$ , Table I) indicates substantial decrease of chain mobility of the copolymer due to the high dipolar character of the structural unit (cyano groups).<sup>17,30</sup> Similar result was observed in the case of poly(AN-co-vinyl acetate) copolymer since the corresponding  $T_g$  was  $86^\circ\text{C}$ <sup>15,16</sup> ( $T_g(\text{poly(vinyl acetate)})=32.6^\circ\text{C}$ ).<sup>31</sup>

Generally, the  $T_{gs}$  of copolymers of MAN were higher than those of the copolymers of AN because of the steric effect of methyl group replacing H in AN comonomer.<sup>15</sup> However, in our case, the  $T_g$  of poly(AN-co-CVA) copolymer was higher than that of poly(MAN-co-CVA) copolymer. This could be explained by the possible high incorporation ratio of CVA unit in AN copolymer (63%) comparatively to that in the MAN copolymer (44%). This increased the interaction between the main chains due to the

strong cyano groups of CVA in the copolymer backbone.<sup>19,21,22</sup>

Information on the thermal decomposition of the homo and the copolymers of CVA was obtained from thermogravimetric analysis under nitrogen. The thermogram recorded in Figure 4 showed that the thermal degradation behaviors of poly(AN-co-CVA), poly(MAN-co-CVA) copolymers and poly(CVA) homopolymer, occurred in a single stage. Table I summarizes the degradation temperatures  $T_d$  and  $T_d'$  corresponding to 1% and 10% of weight loss, respectively. It is noted that the incorporation of cyano monomers, such as AN and MAN, in the copolymers based on CVA improves the thermal stability of the poly(CVA) homopolymer. The poly(AN-co-CVA) and poly(MAN-co-CVA) copolymers started to decompose from 208 and  $212^\circ\text{C}$ , respectively, corresponding to 1% of weight loss. Similar result was observed in the thermal degradation of the copolymers of methyl  $\alpha$ -acetoxyacrylate (MAA) with AN and MAN as comonomers, with the thermal decomposition of poly(AN-co-MAA) and poly(MAN-co-MAA) copolymers occurring at  $180^\circ\text{C}$  and  $240^\circ\text{C}$ , respectively.<sup>32</sup> The weight loss at the end of the programming temperature ( $550^\circ\text{C}$ ) of the polymers of CVA was in the range 53–68 % (Fig. 4). The main volatile products of pyrolysis should be acetic acid and monomers (CVA and MAN) obtained from an elimination reaction from the acetoxy group of CVA units and depolymerisation process respectively. Indeed, the analysis by coupled gas chromatography-mass spectroscopy of the majors products of pyrolysis of poly(vinylidene cyanide-co-CVA),<sup>33</sup> poly(AN-co-MAA) and poly(MAN-co-MAA) copolymers volatile products were acetic acid, CVA and MAN monomers.<sup>32</sup>

### Dielectric behavior

The dielectric spectra were recorded for poly(AN-co-CVA), poly(MAN-co-CVA) copolymers and poly(CVA) homopolymer.

For dielectric measurements, Figure 5 shows the real permittivity  $\epsilon'$  [Fig. 5(a)] and imaginary part  $\epsilon''$  [Fig. 5(b)], respectively, as functions of temperature for the following seven frequencies: 0.1, 1, 10, 100, 1000, 10,000, and 10,000 Hz for a typical dielectric behavior of the poly(MAN-co-CVA) copolymer.

Two successive parts can be pointed out from the analysis of  $\epsilon'$  and  $\epsilon''$  according to the temperature zone: the first from 30 to  $120^\circ\text{C}$  and the second from 120 to  $170^\circ\text{C}$ .

In the temperature range 30 to  $120^\circ\text{C}$ ,  $\epsilon'$  and  $\epsilon''$  had low dependence on the frequency (0.1 Hz to 100 kHz). Generally, in this range at Sub- $T_g$  temperatures and frequencies weak relaxation process  $\beta$  is observed in the range temperature ( $80\text{--}90^\circ\text{C}$ ).<sup>34</sup> It

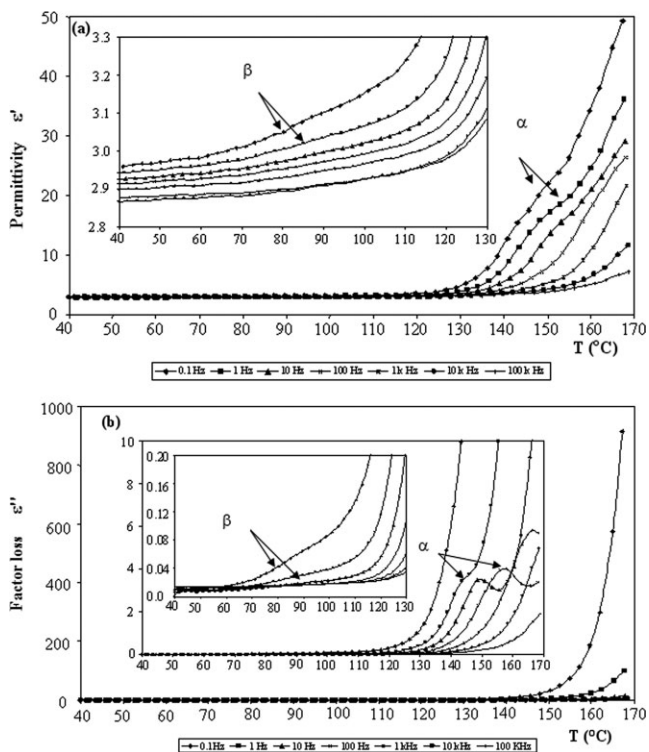


**Figure 5** The dielectric permittivity  $\epsilon'$ (a) and the loss factor  $\epsilon''$ (b) versus temperature of poly(MAN-co-CVA) copolymer at various frequencies.

was assigned to orientation of small dipoles such as  $\text{OCOCH}_3$  of CVA for example.<sup>35,36</sup> Segmental mobility of the polymer molecules increased with temperature, leading to the increase in real part of the permittivity  $\epsilon'$ .

For 120 to 170°C (above  $T_g$ ), the dielectric spectra showed a relaxation phenomenon. This second relaxation phenomenon known under the name of  $\alpha$  relaxation can not be explained if one simply considers free of independent cyano dipoles.<sup>10</sup> This primary relaxation was associated to the cooperative movements of the polar groups (CN) at the time of the mobility of the principal chains as it was observed in common amorphous polymers based on VCN,<sup>10,11</sup> methyl vinylidene cyanide MVCN,<sup>18</sup> AN and MAN.<sup>37,38</sup> The relaxation peak was shifted to high frequency when the temperature increased due to faster molecule movements leading to the decrease in the relaxation times.<sup>39</sup> At very low frequencies (0.1, 1, and 10 Hz) and high temperatures (above 140°C) (Fig. 5), the additional effect of the electrode polarization brings the permittivity  $\epsilon'$  and dielectric loss  $\epsilon''$  to very high values, it was attributed to free building between the sample and the electrodes, indicating conduction process.<sup>40,41</sup>

To minimize the effects of the polarization of electrode, the formalism of electric modulus using  $M^*$  is introduced. This additional analysis has been

recently adapted for the investigation of dielectric processes occurring in composite polymeric systems and also proposed for the description of systems with ionic conductivity.<sup>34,42,43</sup> In analogy to mechanical relaxation, the electric modulus  $M^*$  is defined by the following equation<sup>44</sup>:

$$M^* = \frac{1}{\epsilon^*} = \frac{1}{\epsilon' - j\epsilon''} = \frac{\epsilon'}{\epsilon'^2 + \epsilon''^2} + j \frac{\epsilon''}{\epsilon'^2 + \epsilon''^2} = M' + jM'' \quad (2)$$

where  $M'$  is the real and  $M''$  the imaginary electric modulus.

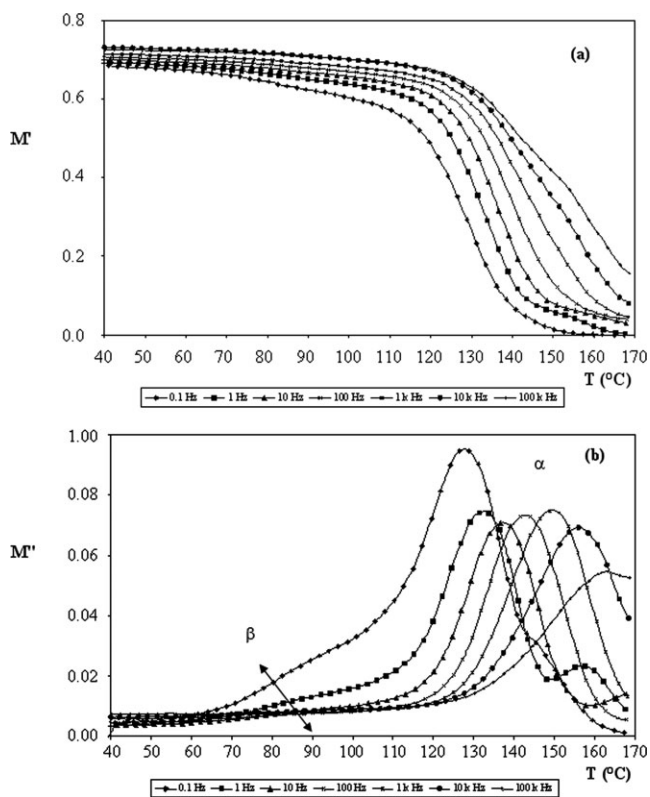
Adopting the electric modulus, Figure 6 shows the variation of the real  $M'$  and the imaginary  $M''$  parts of the electric modulus in isochronal way. Relaxation peaks were clearly formed and a further study and analysis become possible, compared to the representation according to the real and imaginary parts of the complex permittivity  $\epsilon^*$ .

From Figure 6(a), it can be clearly seen that values of  $M'$  take a rather constant value in the low temperature domain (40–70°C), then decreased when temperature increased at a constant frequency. In the temperature range of measurements, relaxation peaks in the values of  $M''$  [Fig. 6(b)] were developed, indicating the relaxation process. Increasing the frequency shifted the peak  $M''$  to higher temperatures.

A series of three distinct phenomena can be considered as the sample is heated over the whole temperature range (Fig. 6). The first of them is related to the  $\beta$  relaxation as indicated above. The sample being at a temperature above the  $\beta$  relaxation, we noted a fast increase in  $M''$  until reaching a maximum of loss. On the other hand, very large absorption relaxation peaks suddenly emerged around the  $T_g$  ( $T = 124^\circ\text{C}$ ). This second phenomenon ( $\alpha$  relaxation) is assigned to the glass transition of the polymer. Segmental mobility of the polymer molecules increased with temperature, leading to the increase in permittivity, i.e., the decrease of the real part of the electric modulus.

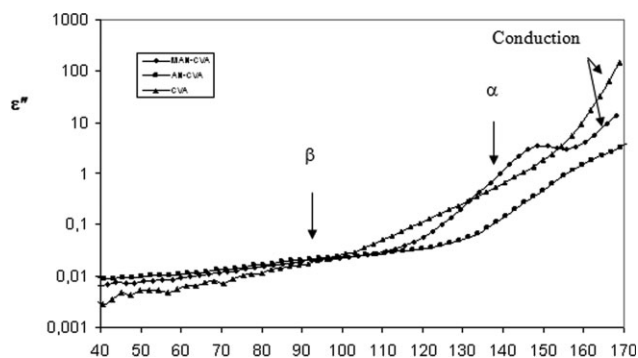
A last phenomenon, which is only noted at high temperatures and low frequencies, especially for the poly(MAN-co-CVA) [Fig. 6(b)], is associated to conductivity effects (due to the drift of ionic impurities).<sup>11,18</sup> The shoulder, related to this phenomenon, shifts to lower frequencies (i.e., at 1 Hz, 10 Hz) with decreasing temperature.

Figure 7 shows a comparison of the loss factor values ( $\epsilon''$ ) of material (copolymers and homopolymer) versus the temperature at 10 Hz. This figure shows that the dielectric behavior of these polymers (poly(CVA) homopolymer and poly(AN-co-CVA) copolymer) presented the same phenomenon as poly(MAN-co-CVA) copolymer. It means that the temperature range can be divided into three regions:



**Figure 6** Isochronal curves of the real part  $M'$ (a) and imaginary part  $M''$ (b) of the dielectric modulus versus temperature of poly(MAN-co-CVA) copolymer.

(i) below  $T_g$ , some changes of  $\epsilon''$  can be found with  $T$  in the range temperature (80–90°C) due to the presence of a weak secondary  $\beta$  relaxation; (ii) above  $T_g$ , molecular dipoles were able to orient under the external field. It was related to  $\alpha$  relaxation phenomena, which have also been characterized around the  $T_g$  of each polymer. In the case of poly(CVA) and poly(AN-co-CVA) polymers, these  $\alpha$  relaxations overlap at high temperature above  $T_g$  and low frequency (10 Hz) by DC conduction. This last one is responsible for the very high values of the real and imaginary part of the dielectric function.<sup>45</sup>



**Figure 7** Dielectric spectra of the variation of the loss factor  $\epsilon''$  versus temperature at 10 Hz for poly(CVA) and poly(AN-co-CVA) polymers compared with the poly(MAN-co-CVA) copolymer.

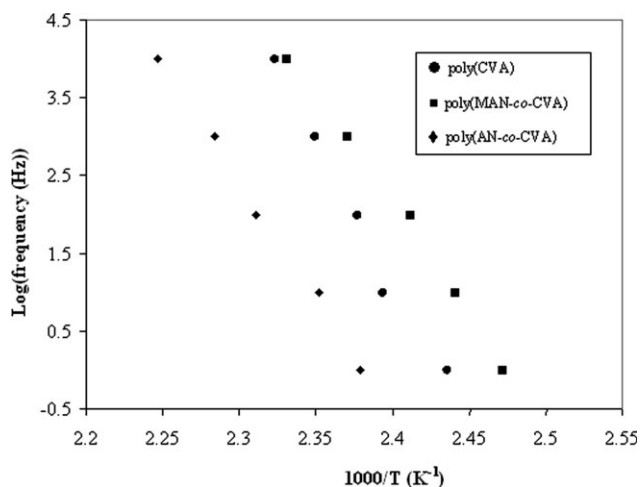


**Figure 8** Arrhenius plots of the frequency of the  $M''$  maximum versus the reciprocal temperature for the different samples.

To determine the relaxation rate of  $\alpha$  relaxation, the activation energy was evaluated using the Arrhenius relation [eq. (3)]:

$$f = f_0 \exp\left(-\frac{E_a}{k_B T}\right) \quad (3)$$

where  $f_0 = 1/2\pi\tau_0$ ,  $f$  being the frequency at which  $M''$  maxima occurs,  $E_a$  is the activation energy and  $k_B$  the Boltzmann constant. According to the range of frequency of the present analysis (10<sup>-1</sup> Hz to 100 kHz), relaxation map (Fig. 8) showed a linear variation of the  $\log f$  versus  $1/T$  from that was used to calculate the apparent activation energy for comparison.

The temperature dependence of the relaxation time for  $\alpha$  relaxation cannot be described or fitted by the Vogel-Fulcher–Tammann (VFT) eq. (4)<sup>46</sup>:

$$\tau(T) = \tau_0 \exp\left(\frac{E_a}{R(T - T_V)}\right) \quad (4)$$

where  $R$  is the gas constant,  $\tau_0 = 1/2\pi f_0$  and  $T_V$  is the Vogel temperature, where ideally the relaxation time should diverge. In fact the  $\alpha$  process shows an Arrhenius behavior corresponding to  $T_V = 0$  as the relaxation map showed a linear variation of the  $\log f$  versus  $1/T$  (Fig. 8).

The values of the apparent activation energy were 574, 538, and 523 kJ mol<sup>-1</sup> for the poly(AN-co-CVA), poly(MAN-co-CVA), and poly(CVA) polymers, respectively. These energies, around a few hundreds of kJ mol<sup>-1</sup>, confirm that it is concerning a primary relaxation phenomenon associated with the glass transition of the copolymers. Similar values of the activation energies were obtained in common amorphous polymers such poly(alkyl methacrylate)s (about 300–500 kJ mol<sup>-1</sup>)<sup>47</sup> and the copolymers



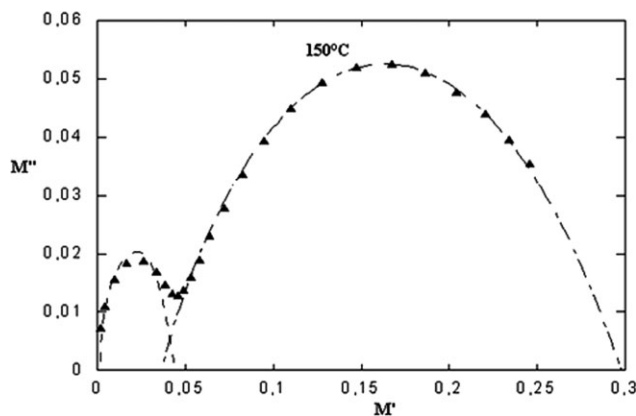


**Figure 9** Argand's plots of the electric modulus,  $M^*$  of the poly(MAN-co-CVA) copolymer at 150°C. The dotted curves are produced by best fitting experimental points to the Havriliak–Negami equation (◆: experimental points (-: theoretical curve).

based on cyanide monomers.<sup>10–12,18</sup> The  $\alpha$  relaxation requires apparent activation energy relatively significant so that the dipoles CN can be oriented in the direction of the applied electric field. Because of strongly polar groups, high forces of interchains are established and needs significant energies to allow orientation of CN groups.<sup>18</sup>

Isothermal dielectric experiments were also performed of poly(MAN-co-CVA) copolymer for frequencies varying from 0.1 Hz to 100 kHz. These isothermal experiment has been frequently used to examine the effect of the relaxation on the value of the  $\epsilon'$  by looking at the value of the dielectric increment  $\Delta\epsilon$  around  $T_g$  determinate by Cole–Cole diagram. According to the theory of Onsager,<sup>48</sup> the dielectric relaxation strength  $\Delta\epsilon$  is proportional to the number of dipole being directed in the field applied.

The use of the Argand representation (Cole–Cole diagram) provides interesting information regarding the nature of the relaxation. A Cole–Cole plot of poly(MAN-co-CVA) copolymer at 150°C is shown in Figure 9.

The dotted curves were produced by best fitting experimental points to the Havriliak–Negami equation<sup>49</sup>:

$$\epsilon^*(\omega) = \epsilon_\infty + \frac{\epsilon_s - \epsilon_\infty}{(1 + (i\omega\tau)^\gamma)^\beta} = \epsilon_\infty + \frac{\Delta\epsilon}{(1 + (i\omega\tau)^\gamma)^\beta} \quad (5)$$

where  $\epsilon_s$  and  $\epsilon_\infty$  are the dielectric constants on the low- and high-frequency sides of the relaxation,  $\tau$  is

the central relaxation time,  $\omega$  is the radial frequency, and  $\gamma$  and  $\beta$  are fractional shape parameters describing the skewing and broadening, respectively, of the dielectric function. Both  $\gamma$  and  $\beta$  range between 0 and 1. The coefficient  $\gamma$  and  $\beta$  are a measure of the deviation from the Debye equation. In fact, when  $\gamma = 1$  and  $\beta = 1$ , this equation reduces to the Debye equation.

In the electric modulus formalism the Havriliak–Negami equation have the following form<sup>39</sup>:

$$M' = \frac{\epsilon'}{\epsilon'^2 + \epsilon''^2} = M_\infty M_s \frac{M_s D_1^2 + D_1 D_2 \cos \beta\phi}{M_s^2 D_1^2 + D_2 [D_2 + 2M_s D_1 \cos \beta\phi]} \quad (6)$$

$$M'' = \frac{\epsilon''}{\epsilon'^2 + \epsilon''^2} = M_\infty M_s \frac{D_1 D_2 \sin \beta\phi}{M_s^2 D_1^2 + D_2 [D_2 + 2M_s D_1 \cos \beta\phi]} \quad (7)$$

where

$$M_s = 1/\epsilon_s; M_\infty = 1/\epsilon_\infty;$$

$$D_1 = (\cos \phi)^\beta \left[ 1 + (\omega\tau)^{2\gamma} + 2(\omega\tau)^\gamma \sin \frac{\gamma\pi}{2} \right]^\beta$$

$$D_2 = (M_\infty - M_s) \left[ 1 + (\omega\tau)^\gamma \sin \frac{\gamma\pi}{2} \right]^\beta$$

$$(\omega\tau)^\gamma = \frac{\tan \left[ \frac{1}{\beta} \arctan \left[ \frac{M_\infty M''}{M_\infty M' - M''^2 - M^2} \right] \right]}{\cos \frac{\gamma\pi}{2} - \sin \frac{\gamma\pi}{2} \tan \left[ \frac{1}{\beta} \arctan \left[ \frac{M_\infty M''}{M_\infty M' - M''^2 - M^2} \right] \right]}$$

From the fitting curves produced (Fig. 9), we can note that:

1. For the data at low frequencies (low  $M'$ ), we obtained a Debye behavior where the experimental points were fitted by a semicircle ( $\gamma = \beta = 1$ ). They are only related to electrode polarization effects. Similar result was found in the previous work.<sup>40</sup>
2. At higher frequencies, the  $\alpha$  relaxation makes an additional contribution to  $M''$ .

The parameters evaluated at 150°C from the fitting procedure of all polymers are listed in Table IV. The

**TABLE IV**  
Parameters Evaluated by Fitting Data According to the Havriliak–Negami Equation for Poly(CVA) and Poly(MAN-co-CVA) and Poly(AN-co-CVA) Copolymers at 150°C

Samples	Relaxation	$\gamma$	$\beta$	$M_s$	$M_\infty$	$\Delta\epsilon = \frac{1}{M_s} - \frac{1}{M_\infty}$
Poly(CVA) 150°C	$\alpha$	0.43	0.98	0.058	0.412	14.81
Poly(AN-co-CVA) 150°C	$\alpha$	0.35	0.98	0.039	0.474	23.53
Poly(MAN-co-CVA) 150°C	$\alpha$	0.60	0.81	0.042	0.29	20.36

$\gamma$  and  $\beta$  values corresponded to pure Debye type for the polarization and did not correspond to a single relaxation time process or a pure Debye-type relaxation.<sup>50</sup>

We note that the value of  $\Delta\epsilon$  of the polymers of CVA listed in Table IV was higher than that of amorphous polymers such as the poly(acetoxymethylstyrene)s for which the value of the dielectric increment lied between 0.4 and 0.9,<sup>51</sup> the poly(vinyl acetate) ( $\Delta\epsilon = 6.5$  at 40°C),<sup>52</sup> the poly(VCN-*alt*-4-chlorostyrene) ( $\Delta\epsilon = 13.1$  at 171.6°C)<sup>11</sup> and the poly(MVCN-*co*-4-fluorostyrene) ( $\Delta\epsilon = 10.9$  at 197.2°C).<sup>18</sup> Extremely large relaxation strength above  $T_g$  means the presence of the cooperative movements implying the movements of orientation of large segments (dipoles CN) at temperatures above  $T_g$  as suggested by Furukawa et al.<sup>53</sup> It means that  $\Delta\epsilon$  is proportional to the density of the aligning cyano dipoles in the direction of the field applied<sup>10</sup> and gives also information about the polarity of the polymer.<sup>54</sup> In the case of the samples studied in this work, the incorporation of MAN in poly(MAN-*co*-CVA) increased the density of cyano dipoles (the dielectric relaxation strength  $\Delta\epsilon$ ) comparatively to that of poly(CVA) ( $\Delta\epsilon = 18.04$ ). We note also that the poly(MAN-*co*-CVA) ( $\Delta\epsilon = 24.42$ ) was more polar than poly(AN-*co*-CVA) ( $\Delta\epsilon = 14.83$ ). This hypothesis was confirmed by a calculation of dipole moments made for propane nitrile and isobutyronitrile, which gave 2.97 Debye and 3.01 Debye, respectively, using a Chem3D<sup>®</sup> software from the CambridgeSoft Corporation.<sup>38</sup> Several factors utilizing the mobility of the chain and the modes of orientation of CN dipoles at the time of the relaxation could be considered,<sup>9,10</sup> the orientation of dipoles needs a free volume to be aligned.<sup>18</sup> Hence, the voluminal polarity is weaker in the case of poly(AN-*co*-CVA). This low flexibility of the chain in poly(AN-*co*-CVA) limits the reorientation of the CN groups in the direction of the applied electric field thus reducing the value of the dielectric relaxation strength  $\Delta\epsilon$ .

## CONCLUSIONS

New random copolymers containing  $\alpha$ -cyanovinylacetate and cyano comonomers (AN, MAN) were synthesized by radical copolymerization initiated by AIBN. These copolymers were characterized by <sup>13</sup>C NMR and IR spectroscopy. The copolymer compositions were determined by NMR spectroscopy, the molar percentages of incorporation of AN and MAN in the copolymers were 36% and 56%, respectively. The microstructures of the copolymers were also studied using some characteristic signals in <sup>13</sup>C NMR spectra. The statistical structure of poly(AN-*co*-CVA) copolymer is in good agreement with the calculated values of reactivity ratios. DSC and

TGA showed that the copolymers were amorphous with a high  $T_g$  and stable up to 200, 208, and 212°C for poly(CVA), poly(AN-*co*-CVA), and poly(MAN-*co*-CVA), respectively. Using dielectric spectroscopy, we have studied the dielectric properties of these polymers. Dielectric weak relaxation  $\beta$  at sub- $T_g$  temperatures was observed usually originating from molecular motions that are restricted to the scale of few bond lengths. Strong  $\alpha$  relaxation processes occurred above the  $T_g$ . This primary relaxation was associated to the cooperative movements of the polar groups (CN) of the main chains. The intensity of relaxation were evaluated at 150°C from the fitting curves produced using the Havriliak–Negami equation. These values show the potential application of such materials in the domain of electronics.

## References

1. Guilbert, H.; Miller, F. F.; Averill, S. J.; Carlson, E. J.; Folt, V. L.; Heller, H. J.; Stewart, F. D.; Trumbull, H. L. *J Am Chem Soc* 1956, 78, 1669.
2. Conciatori, A. B.; Trapasso, L. E.; Stockmann, R. *Vinylidene cyanide Polymers Encyclopedia of Polymer Science et Technology*; Interscience Publishers: New York, 1971; 14: 580 pp.
3. Miyata, S.; Yoshikawa, M.; Tasaka, S.; Ko, M. *Polym J* 1980, 12, 857.
4. Maruyama, Y.; Yo, Y. S.; Inoue, Y.; Chujo, R.; Tasaka, S.; Miyata, S. *Polymer* 1987, 28, 1087.
5. Inoue, Y.; Kawaguchi, K.; Maruyama, Y.; Yo, Y. S.; Chujo, R.; Seo, I.; Kishimoto, M. *Polymer* 1989, 30, 698.
6. Inoue, Y.; Kashiwaki, A.; Maruyama, Y.; Yo, Y. S.; Chujo, R.; Seo, I.; Kishimoto, M. *Polymer* 1988, 29, 144.
7. Montheard, J. P.; Boinon, B.; Belfkira, A.; Raihane, M.; Pham, Q. T. *Makromol Chem* 1993, 194, 2839.
8. Ohta, Y.; Inoue, Y.; Chujo, R.; Kishimoto, M.; Seo, I. *Polymer* 1990, 31, 1581.
9. Sakurai, M.; Otha, Y.; Inoue, Y.; Chujo, R. *Polymer* 1991, 32, 197.
10. Zou, D.; Iwasaki, S.; Tsutsui, T.; Saito, S.; Kishimoto, M.; Seo, I. *Polymer* 1990, 31, 1888.
11. Belfkira, A.; Sadel, A.; Montheard, J. P.; Boiteux, G.; Lucas, J. M.; Seytre, G. *Polymer* 1993, 34, 4015.
12. Inoue, Y.; Jo, Y. S.; Kashiwazaki, A.; Maruyama, Y.; Chujo, R.; Kishimoto, M.; Seo, I. *J Polym Comm* 1988, 29, 105.
13. Kishimoto, M.; Seo, I.; Fujimoto, Y. EP 04150342, 1990. Mitsubishi Petrochemical Chem Abstr 1990, 109, 009621.
14. East, A.; Conciarto, A. B. WO 91/ 13922, 1991. Hoechst Celanese PCT. Chem Abstr 1991, 116, 7371.
15. Padias, A. B.; Chu, G.; Kalnin, I.; Hall, H. K. Jr. *Polym Repr* 1991, 32, 537.
16. Hall, H. K. Jr, Padias, A. B.; Chu, G.; Lee, H. Y.; Kalinin, I.; Sansone, M.; Breckenridge, G. *J Polym Sci Part A: Polym Chem* 1992, 30, 2341.
17. Montheard, J. P.; Boinon, B.; Raihane, M.; Pham, Q. T. *Polym Commun* 1991, 32, 567.
18. Raihane, M.; Montheard, J. P.; Boiteux, G. *Macromol Chem Phys* 2000, 201, 2365.
19. Montheard, J. P.; Mesli, A.; Belfkira, A.; Raihane, M. *Macromol Rep* 1994, 1.
20. Tanaka, H.; Okazaki, T.; Tezuka, Y.; Hongo, T.; Takahashi, Y. *Polymer* 2002, 43, 1189.
21. Montheard, J. P.; Zerroukhi, A.; Ouillon, I.; Raihane, M. *J Macromol Sci Part A: Pure App Chem* 1997, 34, 291.

22. Raihane, M.; Ameduri, B. *J Fluorine Chem* 2006, 127, 391.
23. Tadatoshi, O.; Masahiro, K.; Akira, O. *Kogyo Kagaku Zasshi* 1968, 71, 899.
24. Weir, M. R. S.; Hyne, J. B. *Can J Chem* 1963, 41, 2905.
25. Pham, Q. T.; Petiaud, R.; Waton, H.; Lauros-Darricades, N. F. *Proton and Carbon NMR Spectra of Polymer*; Prenton Press: New-York, 1991.
26. Montheard, J. P.; Zerroukhi, A.; Ouillon, I.; Raihane, M.; Pham, Q. T. *Polym Bull* 1996, 36, 709.
27. Alfrey, T.; Price, C. C. *J Polym Sci* 1974, 2, 101.
28. Greenley, R. Z. *J Macromol Sci Chem* 1975, 9, 505.
29. Tadatoshi, O. *Enka Biniiru to Porima* 1968, 8, 26.
30. Kharas, G. B.; Feinberg, C. B. *Polym Prepr (Am Chem Soc Divi PolyChem)* 1988, 29, 180.
31. Daniels, W. Mark, H. F., Ed. In *Encyclopedia of Polymer Science and Technology*, Wiley-Interscience: New York, 1987; Vol 17, 402 pp.
32. Ouillon, I.; Raihane, M.; Zerroukhi, A.; Boinon, B. *Macromol-Chem Physic* 1997, 198, 3425.
33. Raihane, M.; Lalèque, N.; Boinon, B. *Thermochim Acta* 1995, 265, 1.
34. Wubbenhous, M. *J Non Crystalline Solids* 2002, 305, 40.
35. Soares, B. G.; Leyva, M. E.; Barra, G. M. O.; Khastgir, D. *Eur Polym J* 2006, 42, 676.
36. Murthy, S. S. N.; Shahin, M. d. *Eur Polym J* 2006, 42, 715.
37. Raihane, M.; Kallel, A.; Arous, M.; Kaddami, H. Results presented at the International Meeting of Material for Electronic Applications "IMMEA"; Marrakech, Morocco, April 30–May 2, 2007; 95 pp.
38. Meskini, A.; Raihane, M.; Ameduri, B.; Hakme, C.; Sage, D.; Stevenson, I.; Boiteux, G.; Seytre, G.; Kaddami, H. *Eur Polym J* 2009, 45, 804.
39. Tsangaris, G. M.; Psarras, G. C.; Kontopoulos, A. J. *J Non Crystalline Solids* 1991, 131, 1164.
40. Hammami, H.; Arous, M.; Lagche, M.; Kallel, A. *Compos part A* 2006, 37, 1.
41. Capaccioli, S.; Raihane, M.; Castelvetro, V.; Meskini, A.; Atlas, S. Results presented at the International Meeting of Material for Electronic Applications "IMMEA"; Marrakech (Morocco, April 30–May 2, 2007; 29 pp.
42. Arous, M.; Kallel, A.; Fakhfakh, Z.; Perrier, G. *J Phys Soc Jpn* 1997, 66, 3665.
43. Mccrum, N. G.; Read, B. E.; Williams, G. *Anelastic and dielectric effects in polymeric solids*; Wiley: London, 1967; 108 pp.
44. Tsangaris, G. M.; Psarras, G. C.; Kouloumbi, N. *J Mater Sci* 1998, 33, 2027.
45. Jonscher, A. K. *J Phys D: Appl Phys* 1999, 32, 57.
46. Vogel, H. Z. *Physik* 1921, 22, 645.
47. Yoshida, H.; Kobayashi, Y. *J Macromo Sci Phys* 1983, 21, 565.
48. Kremer, F.; Schönhals, A., Eds. *Broadband Dielectric Spectroscopy*, Springer-Verlag: Berlin, 2003; Eds
49. Havriliak, S.; Negami, S. *J Polym Sci* 1996, 4, 99.
50. Mudarra, M.; Diaz-Calleja, R.; Belana, J.; Canadas, J. C.; Diego, J. A.; Sellares, J.; Sanchis, M. J. *Polymer* 2001, 42, 1647.
51. Amadei, H.; Monthéard, J. P.; Boiteux, G.; Lucas, J. M.; Seytre, G. *Makromol Chem* 1985, 186, 321.
52. Furukawa, T.; Date, M.; Nakajima, K.; Kokaska, T.; Soe, I. *Jpn J App Phys* 1986, 25, 1178.
53. Furukawa, T.; Nakajima, K.; Kiozimi, N.; Date, M. *Jpn J App Phys* 1987, 26, 1039.
54. Fröhlich, H. *Theory of dielectrics*; Clarendon Press: Oxford, 1958.